IOSR Journal of Applied Geology and Geophysics (IOSR-JAGG)
e-ISSN: 2321–0990, p-ISSN: 2321–0982.Volume 8, Issue 5 Ser. II (Sep. – Oct. 2020), PP 15-26
www.iosrjournals.org

Petrographic and Diagenetic Evaluation of Carbonate Reservoir Quality: A Case study of the Lower Congo Basin, offshore Democratic Republic of Congo

Nadège Mbula Ngoy [1], Agwom Istifanus Madaki [1,2]
[a] *School of Earth Resources, China University of Geosciences, 430074, Wuhan, Peoples Republic of China*
[b] *Department of Geology, University of Jos, P.M.B 2084, Jos, Plateau State, Nigeria*

Abstract
The Lower Congo basin's Albian – Early Cenomanian Pinda group is the most productive carbonate reservoir within the West African margin basins. However, the understanding of its diagenetic features is very limited. Core samples obtained from the Democratic Republic of Congo offshore section of the formation were petrographically analysed to image the sedimentary facies along with diagenetic processes and links to reservoir quality. The sedimentary facies obtained indicate a dominant lagoon sedimentation within the oolitic – siliciclastic ramp. Diagenetic processes detected include micritization, dolomitization, dissolution, cementation, and compaction. Diagenetic links to reservoir quality within the facies is established in the dominant occurrence of moldic pores which have been occluded either by calcite or dolomite cement, leaving three facies with poor reservoir quality. The facie exempted from this class possesses a fair reservoir quality linked to microporosity within its sandstone domain. These observations should serve as important considerations for future reservoir characterization studies within the Pinda group.

Keywords: *Reservoir quality, diagenesis, petrography, Pinda group, Lower Congo basin, offshore Democratic Republic of Congo.*

Date of Submission: 09-10-2020 Date of Acceptance: 25-10-2020

I. Introduction

Carbonate reservoirs make up a large portion of the world's hydrocarbon reservoirs and are characterized by heterogeneities which influence hydrocarbon storage capability. These heterogeneities are due to a variation in depositional environment, diagenesis, and tectonism (Jardine & Wilshart, 1982; Holtz et al., 1992; Ehrenberg et al., 1998; Cerepi et al., 1999; Ehrenberg, 2004; Zou & Tao, 2007; Bera & Belhaj, 2016; Hosa & Wood, 2017; Rashid et al., 2017). Majority of carbonate deposition takes place in tropical shallow marine settings because such environments meet the requirements of abiotic and biotic processes which lead to carbonate rock formation. These requirements or controls on carbonate rock formation include salinity, temperature, and nutrient availability (Schlager, 1999; Singh & Joshi, 2020).

Since diagenetic alteration involves the flow of chemically active fluids through permeable rock (Alsharhan and Magara 1995), high chemical sensitivity of carbonate minerals means they are easily altered during diagenesis thus making diagenetic alteration a major influence on hydrocarbon flow within carbonate reservoirs (Major & Holtz, 1997; Mehrabi & Bonab, 2014). Diagenetic alteration of carbonate rocks results in the acquisition/destruction of various pore types as alteration continues from initial sediment burial to deep burial (Mazzullo, 1994; Saller et al., 1994), and diagenesis influence on flow is also found in its controls on apertures of fractured carbonates (Wennberg et al., 2016).

Porosity – permeability relationships between carbonate reservoirs vary with textures induced by diagenesis (Woody et al., 1996), and fractures (Ehrenberg & Nadeau, 2005; Ehrenberg et al., 2008; Zhou et al., 2018). The porosity developed within a carbonate reservoir varies with diagenesis undergone by each stratigraphic interval (Ehrenberg et al., 1998; Brigaud et al., 2014), and carbonate reservoir pore geometry is diagenetically controlled (Cerepi et al., 2003). Thus, the reservoir quality of a carbonate reservoir can be determined by analysing the evolution of its porosity and permeability with diagenesis.

Over the years, various rock samples have been analysed using different methodologies which includes petrographic analysis of thin sections and isotope analysis (e.g. Nader & Swennen, 2004), which can be combined with an analysis of fluid inclusions/X-ray diffraction (e.g. Ehrenberg et al., 1998; Madi et al., 2000; Lavoie & Chi, 2001; Ehrenberg, 2004; Wierzbicki et al., 2006; Wilson et al., 2007; Machel & Buschkuehle, 2008; Vandeginste et al., 2009) and/or scanning electron microscopic (SEM) imaging and gas injection measurements (e.g. Woody et al., 1996; Bonab et al., 2010; Jiang et al., 2018).

The basins of the West – Central African coast which extend from Cameroon to Namibia are major hydrocarbon provinces with hydrocarbon production from turbidite reservoirs, carbonate platform, and pre-salt reservoirs (Burwood et al., 1995; Brownfield & Charpentier, 2006). Clastic reservoirs have majority of the region's recoverable reserves, followed by carbonate reservoirs of Pinda group in the Lower Congo basin which are ranked sixth amongst hydrocarbon systems in Africa with an estimated 8.2 billion barrels of recoverable oil and gas (Liu et al., 2008). However, due to the proprietary nature of data obtained within the region, knowledge of the carbonate platform's reservoir quality has been limited.

In this study, we used petrographic and SEM imaging, along with routine analysis (porosity, permeability and grain density) of core samples obtained from two exploratory wells, to image the reservoir quality of a carbonate reservoir within offshore Democratic Republic of Congo (DRC). The study also provides insights into the nature of subsurface diagenetic features of carbonate reservoirs within the study area which could provide better information for use in reservoir characterisation and modelling studies.

II. Geologic Setting

The study area which lies within the Lower Congo basin in offshore Democratic of Congo **(Fig. 1a)** belongs to a group of coastal basins within the Western Africa continental margin which formed due to the separation of Gondwana in the Late Cretaceous (Vidal et al., 1975; Valle et al., 2001; Charlou et al., 2004; Moulin et al., 2005; Chaduteau et al., 2009), resulting from the northward rifting of the South Atlantic which began from the Late Jurassic (Nürnberg & Müller, 1991; Eagles, 2007; Torsvik et al., 2009; Moulin et al., 2010; Marcano et al., 2013).

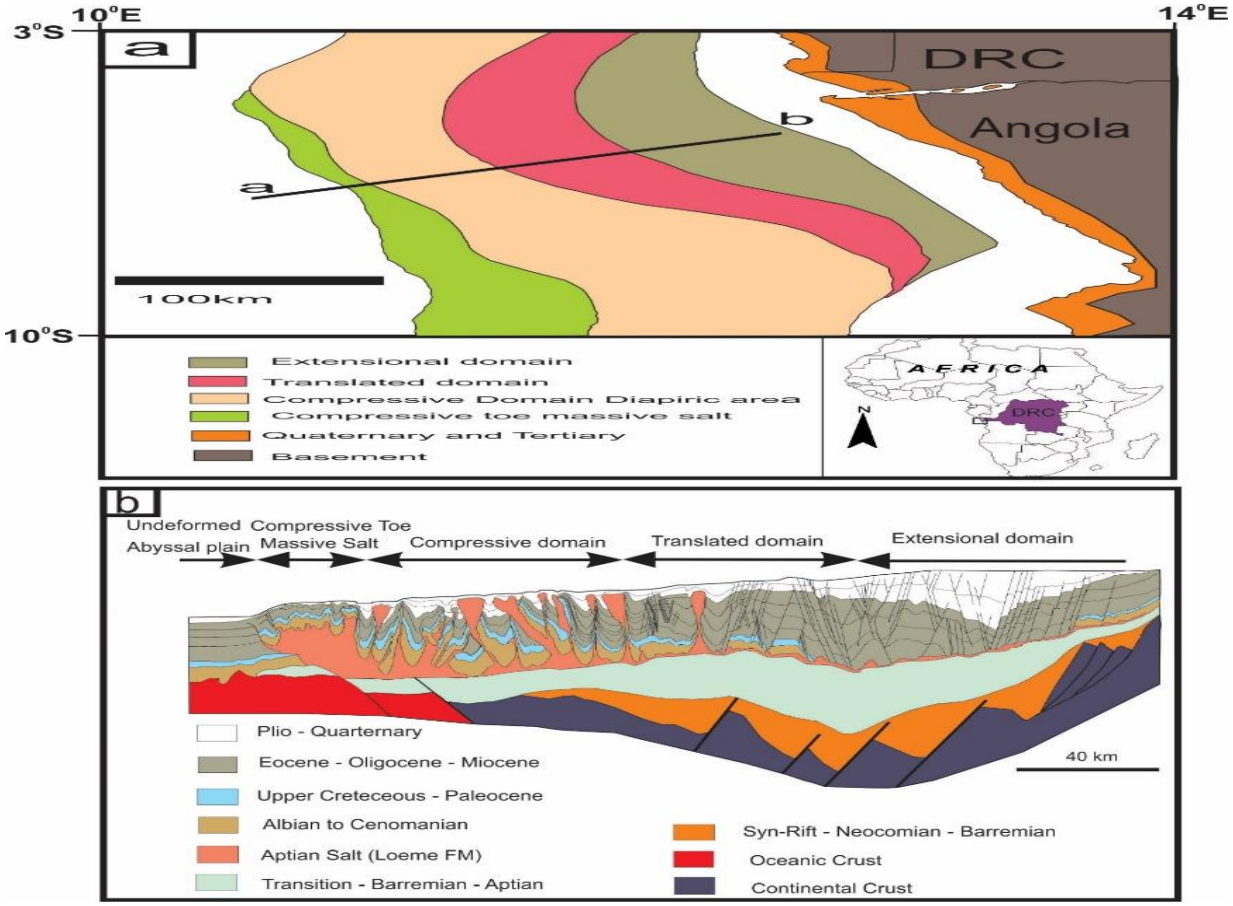

Fig. 1 (a) Geologic map showing regional geologic setting (modified from Leturmy, 2003 and Jatiault et al., 2017). Note location map insert. (b) Lower Congo basin geologic cross-section (a-b in fig 1a) showing basin rift series.

These basins which elongate from the Cameroun volcanic line to the Walvis ridge, are characterized by pre-separation lithology comprising Precambrian basement overlain by Late Jurassic – Aptian terrestrial sediments before rifting caused an invasion of the sea from the South Atlantic which resulted in a transition from continental to marine sediment deposition. These events were then followed by shallow water evaporite deposition due to the Walvis ridge obstruction of seawater invasion as the South Atlantic opened during the

Aptian, and transgressive marine deposition from the Late Aptian (Vidal et al., 1975; Uchupi & Emery, 1975; Ruiter, 1979; Jansen et al., 1984; Moulin et al., 2005**;** Liu & Li, 2011).

Furthermore, there was a post-separation regressive continental sediment deposition in the Cenomanian and extensive marine transgression from the Turonian (Franks and Nairn 1973), to regressive continental deposition as sea levels reduced during the Paleogene (Franks & Nairn, 1973; Vidal et al., 1975; Uenzelmann-Neben et al., 1997; Liu & Li, 2011). While the Oligocene – Miocene was characterized by clastic deposition across the shelf (Cole et al., 2000), subsequent periods were mainly characterized by the development of deep-water turbidite systems (Huang 2018).

The Congo river's control on sedimentation on the Congo – Angola continental margin can be found in the formation of the hydrocarbon rich Congo fan (Holtvoeth et al., 2003; Chaduteau et al., 2009; Baudin et al.,2010), and its underlying sedimentary layer (Anka et al., 2010). Droz & Rigaut, (1996) also attributed renewed continental deposition within the area during the Cenozoic to draining of the Congo river into the Atlantic along with an increase in river bedload transport due to onshore structural deformation and uplift. However, an affirmation of gravity driven tectonics dominance on the area's post-rift deformation and sedimentation (e.g. Valle et al., 2001; Rouby et al., 2003), supports Leturmy, (2003) assertion of climate playing a lesser role. Dickson et al., (2003) also noted the presence of reservoir and source rocks within the margin along with uplift, which were controlled by faults and fractures extending from the mid-ocean ridge. However, Séranne & Anka, (2005) countered the previously stated assertion by positing the influences of climate on sedimentation rate being proven by its positive link to uplift and gravity tectonics within the study area. The interplay between climate and tectonics on source rock and reservoir rock sedimentation within the Lower Congo basin was also supported by subsequent studies (e.g. Lentini et al., 2010; Marcano et al., 2013; Wang et al., 2016; Li et al., 2020).

The evaporite layers in the Lower Congo basin are distributed within the Continental shelf (Liu & Li, 2011), and the basin stratigraphy (**Fig. 2**) attests to a possession of pre-rift, post-rift, syn-rift sediments and Aptian evaporites with the depocenter described by Leturmy, (2003) as migrating from the continental margins to the Congo fan during the Tertiary.

According to Rouby et al., (2003) within the Congo-Angola continental margin; pre-evaporite sedimentation commenced with Lower Carboniferous to Trias-Jurassic fluvio-lacustrine sediments, followed by tectonically active Neocomian to Mid-Barremian clastic sedimentation, overlain by Barremian to Middle Aptian sedimentation. They also described post-evaporite lithology within the study area as commencing with the Lower Albian progradation of a carbonate platform on the Aptian evaporites, before they are episodically overlain by shale and silt during the Upper Albian.

Hydrocarbon generation has been proven in the area's pre-evaporite source rocks (e.g. Burwood et al., 1990; Burwood et al., 1995). The petroleum potential of thick post-evaporite organic rich source rocks within the continental margin has also been positively inferred in some studies (e.g. Uchupi & Emery, 1975; Dickson et al., 2003). Anka et al., (2010) also deduced the study area as being characterized by a basinward decrease in source rock maturity, and Baudin et al., (2010) used the gas prone status of Congo fan sediments to adduce a similar nature for the area's deep sea source rocks. However, while Marcano et al., (2013) described a Palaeocene – Eocene hydrocarbon generation for pre-evaporite source rocks of the Lower Congo basin, Salvi et al., (2013) found an Oligocene – recent oil generation for a deep water pre-evaporite source rock unit. Post-evaporite source rocks are mostly immature with oil-prone Iabe formation as the only one linked with post-evaporite hydrocarbon generation (Cole et al. 2000).

Formation of the Lower Congo basin's post-evaporite hydrocarbon fields is dominated or influenced by salt tectonism **(Fig. 1b)** (Liu & Li, 2011; Oluboyo et al., 2014; Wenau, Spiess et al., 2015; Ge et al., 2019), which also hinders exploitation of its petroliferous pre-evaporite reservoirs (Jameson et al., 2011). Hence, despite good reservoir quality affirmations of the pre-evaporite Toca carbonate formation sealed by the overlying Aptian Loeme salt (see; Beglinger et al., 2012; Frixa et al., 2014), the basin's main carbonate reservoir is the Albian – earliest Cenomanian Pinda group whose hydrocarbons are sourced from the Barremian Bucomazi group (Cole et al., 2000; Liu et al., 2008), and sealed by the overlying Iabe shale **(Fig. 2)**.

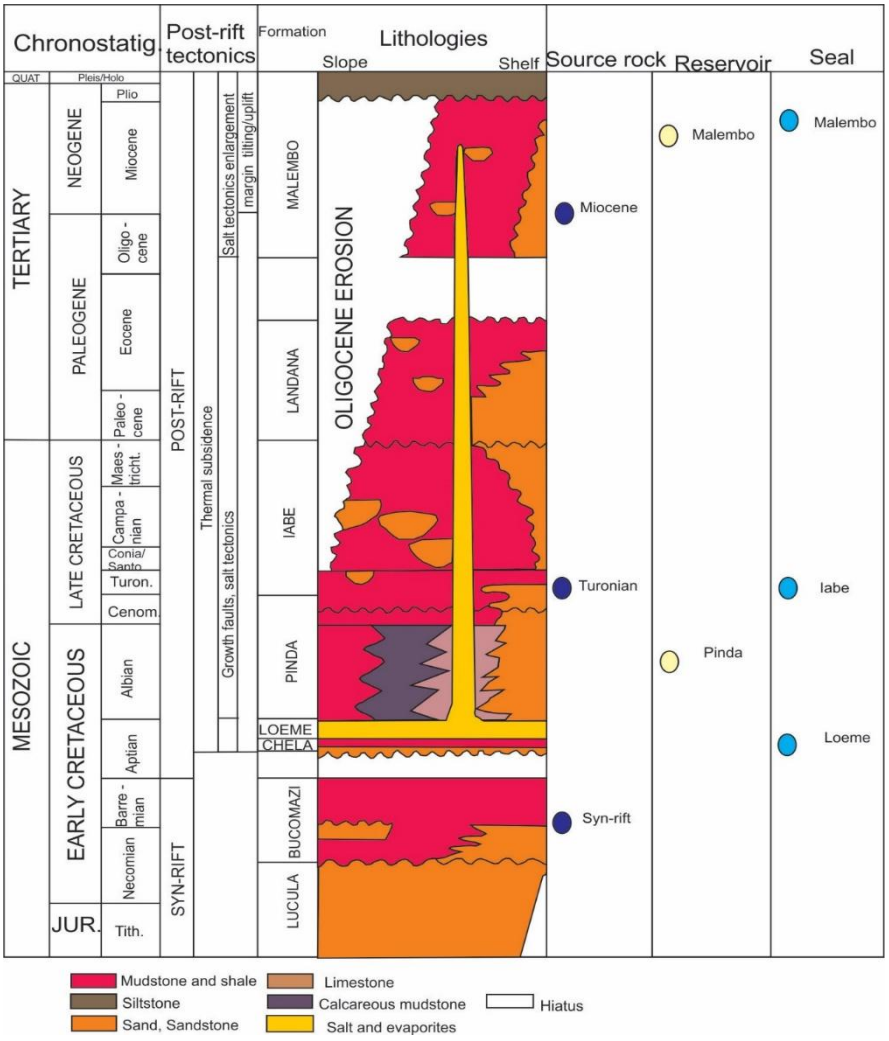

Fig. 2. Lower Congo basin lithostratigraphy (modified from Anka et al., 2009 and Marcano et al., 2013)

This belongs to the post-evaporite carbonate platform which formed due to Northward Albian – Turonian marine deposition on the Aptian evaporites of the West African coastal basins (Brownfield and Charpentier 2006). The Pinda group within the Lower Congo basin is an oolitic-siliciclastic ramp system characterised by both transgressive and regressive tract facies (Eichenseer et al., 1999).

III. Methodology

This study provides preliminary insights into the reservoir quality of a carbonate reservoir in offshore DRC. Core samples were obtained from two exploratory wells with depths sampled based on possible reservoir intervals detected on well logs **(Fig. 3)**. Four core samples were systematically selected for conventional core analysis (CCA), petrographic analysis, Scanning Electron Microscopy (SEM) and X-Ray Diffraction (XRD) analysis (whole rock and clay mineral) all undertaken at a commercial laboratory.

Routine core analysis (RCA) involved porosity measurements undertaken with helium pycnometer via utilization of gas expansion principles, along with permeability and grain density measurements. For whole rock XRD analysis, dried cuttings of the samples were ground before being weighed and micronized at 5 – 10 microns. The resulting slurry was crushed and dried again before being presented to an X-ray beam from a copper anode (at 35kV, 30mA), with samples run between 2° and 60° 2θ at a 0.05°/sec step size. For clay mineral XRD, weighed cuttings were micronized at less than 2 microns before being separated via ultrasound shaking and centrifugation. This was followed by filtering and drying of clay suspension to obtain the XRD mount. The samples were later saturated with ethylene glycol vapor and heated (380°c for 2hrs and 550°c for 1hr) before being scanned with X-ray from a copper anode (at 40kV, 30mA). While first scan was undertaken between 3° and 35° 2θ at a 0.05/sec step size, and the second is done between 24 – 27° 2θ at a 0.02/2sec step size to enhance kaolinite/chlorite peak detection.

For thin section preparation, trims of the samples are impregnated with blue-dyed epoxy resin for pore identification, stained with Alizarin red S and potassium ferrocyanide for carbonate mineral delineation, and sodium cobaltinite for potassium feldspar identification. The Embry & Klovan, (1971) scheme for petrographic analysis, which was modified by Dunham, (1962) was used. The carbonate mineral crystallinities and sorting was obtained from Scholle, (1978), with limestone porosity terms proposed by Choquette & Pray, (1970).

For SEM analysis, sample chips were glued to a mounting stub and coated with gold before presented to a Zeiss Leo 1450VP instrument used to take images with a 20kV backscatter detector, with elemental analysis later done via INCA software.

IV. Results

4.1 LITHOLOGIC FACIES

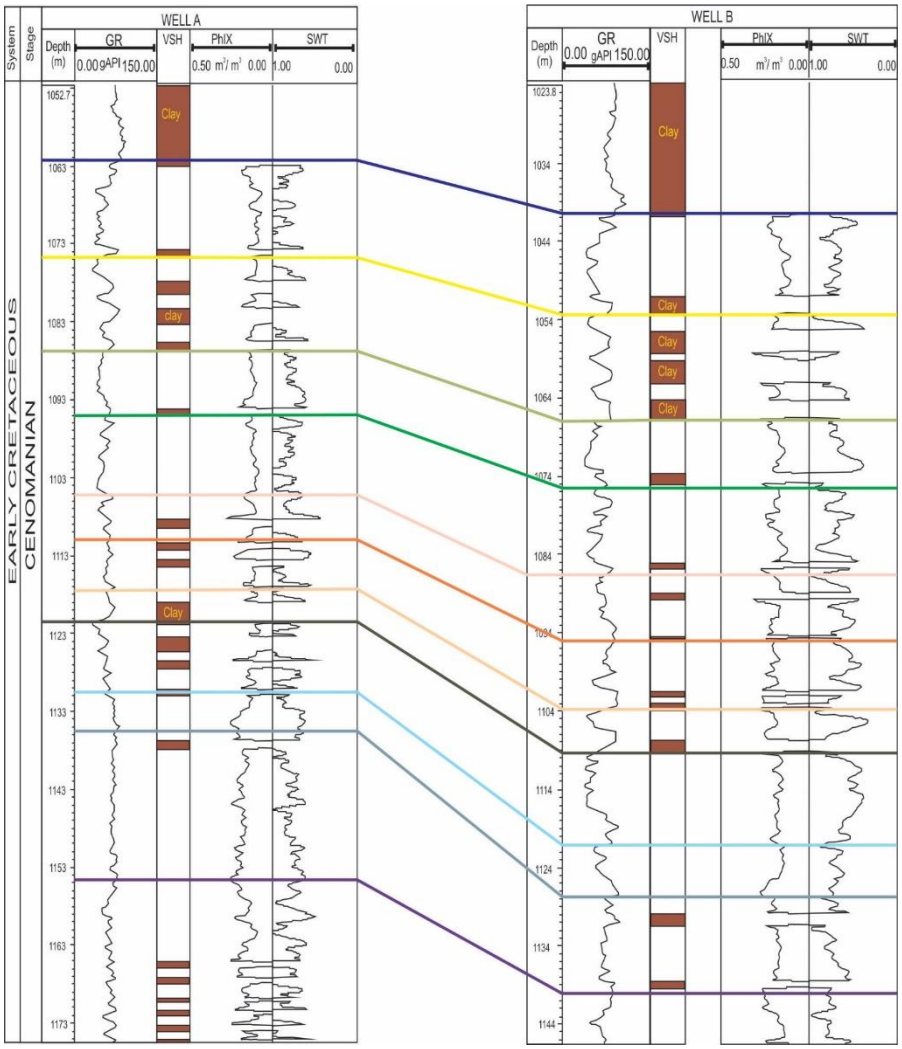

Fig. 3. Correlation of possible reservoir units from the well logs. GR: Gamma ray, VSH: Clay volume, PHIX: Porosity log, SWT: Total water saturation log.

Facie types observed from the core samples include sandy molluscan-metazoan-pelletal packstone, partly recrystallised micritic arkosic sandstone, slightly sandy recrystallized bioclastic wackestone, and sandy molluscan packstone. All carbonate facies were mineralogically dominated by calcite with detrital clastic grains for all samples revealed as consisting quartz, potassium feldspar and plagioclase along with traces of clay minerals **(Fig. 5f, 6c, 6e, 6f)**. Facies detected include Sandy molluscan-metazoan-pelletal packstone, Partly recrystallised micritic arkosic sandstone, Slightly sandy recrystallized bioclastic wackestone, and Sandy molluscan packstone. The facies were mainly characterized by an original micrite matrix which had recrystallized to a non-ferroan calcite microspar, and porosity types which include moldic **(Fig 4c, 5a, 5c, 5e)**, intraparticle **(Fig. 6d, 6f),** intergranular (**Fig. 4d, 6a, 6g),** interparticle **(Fig. 6c, 6f)** and micro-porosity **(Fig. 6a, 6e)**.

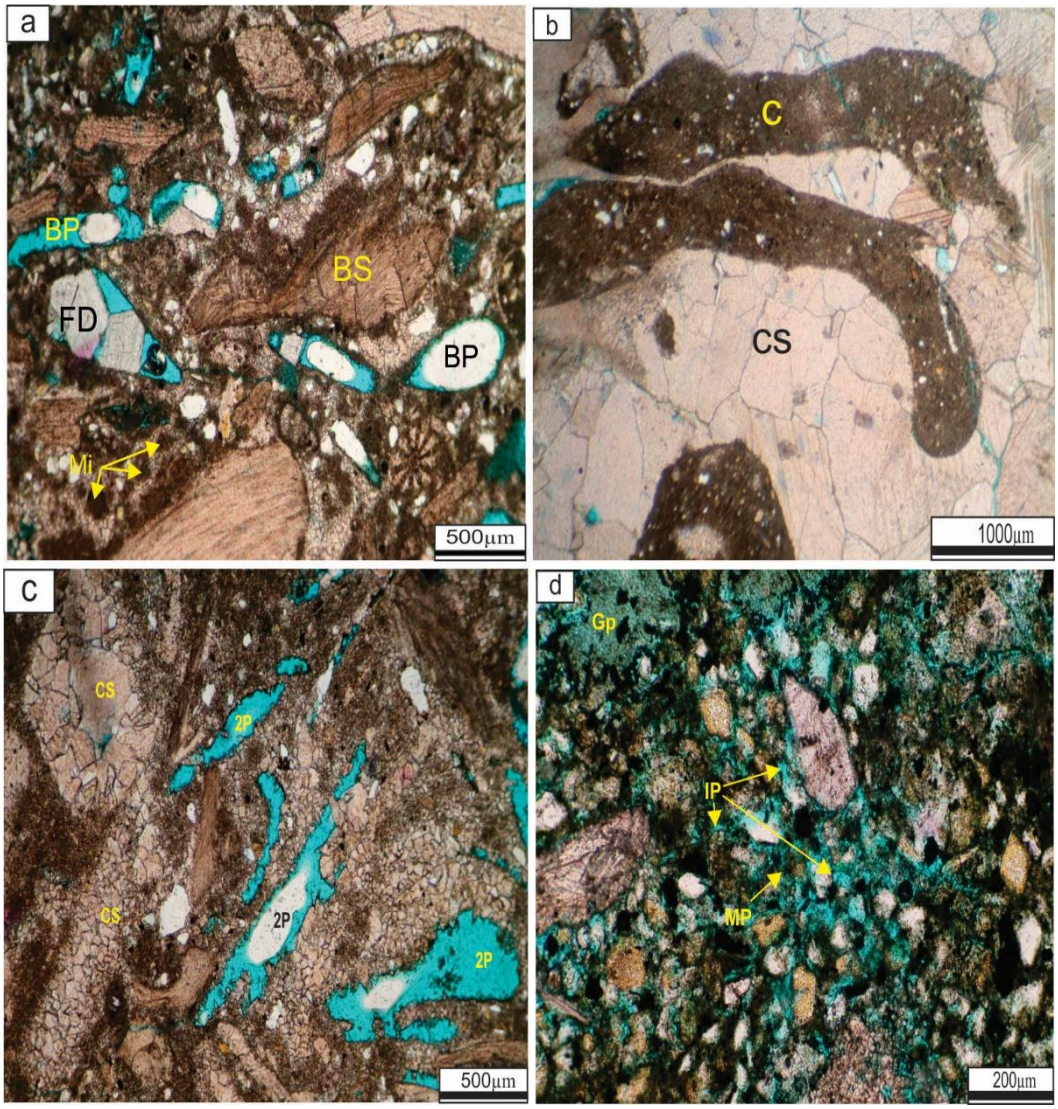

Fig. 4. (a) A packstone domain showing locally common secondary biomouldic porosity (BP) which has been partly infilled by mildly ferroan dolomite (FD) in some cases. Note micrite pellets (Mi), and bivalve shell fragments (BS). (b) A metazoan fragment now consisting of medium non ferroan calcite spar (CS), leaving canal structures (C) originally filled with micrite, and now recrystallized to non-ferroan calcite microspar. (c) Secondary biomouldic porosity (2P) created by the dissolution of bioclasts. Also shows the almost entire occlusion of earlier biomouldic porosity by non-ferroan calcite spar (CS). (d) A sandstone pocket within the sandy molluscan packstone exhibiting primary intergranular porosity (IP) and microporosity (Mp) within its possibly argillaceous patchy matrix. Also shows gypsum as a brine precipitate upon drilling (Gp).

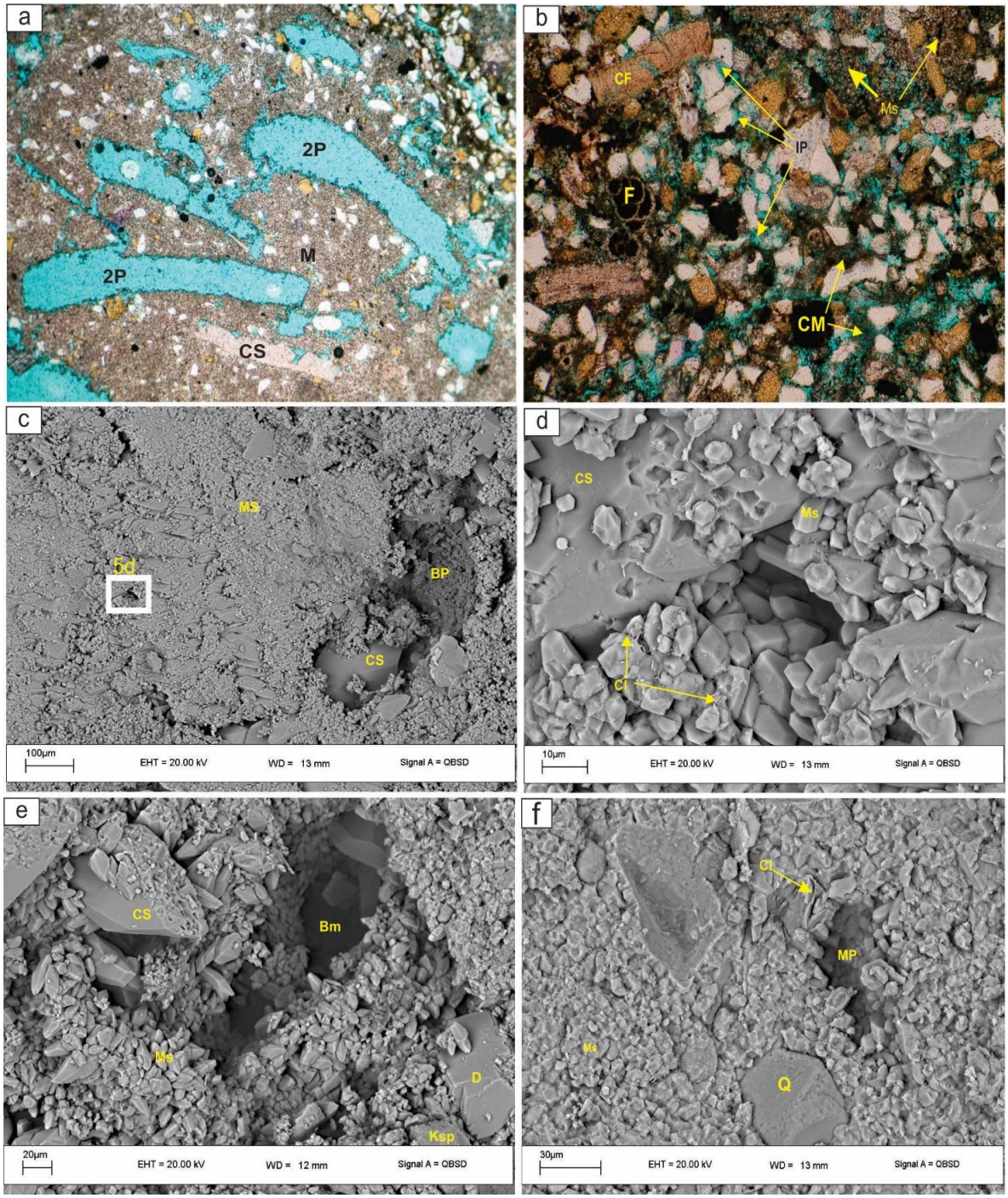

Fig. 5. (a) Locally abundant secondary biomouldic porosity (2P) created by the complete dissolution of mollusc shells, within the recrystallized micrite matrix (M). Note also the local almost complete infilling of this secondary porosity by late stage non ferroan calcite spar crystals (CS). (b) A localised pocket of sandstone displaying primary intergranular porosity (IP). This porosity is seen to be locally partly occluded by a patchy detrital microporous clay matrix (CM). Also note a planktonic foraminifer whose chambers are filled entirely by pyrite and hematite (F), and a collophane fish fragment (CF). The microspar matrix (Ms) is also depicted. (c) An area of recrystallized wackestone composed largely of microspar (MS), hosting biomouldic porosity (BP), partly occluded by medium crystalline calcite spar (CS). (d) Scan showing euhedral microspar (Ms) and later medium crystalline calcite spar (CS), with rare flaky smectitic/illitic clays (Cl). (e) Euhedral calcite microspar (Ms), with later medium crystalline calcite spar (CS) Also shows dolomite (D), detrital K feldspar (Ksp) and a possible biomould (Bm). (f) Compact microspar (Ms) with rare smectitic/ illitic clays (Cl), detrital quartz (Q), and an isolated macropore (Mp).

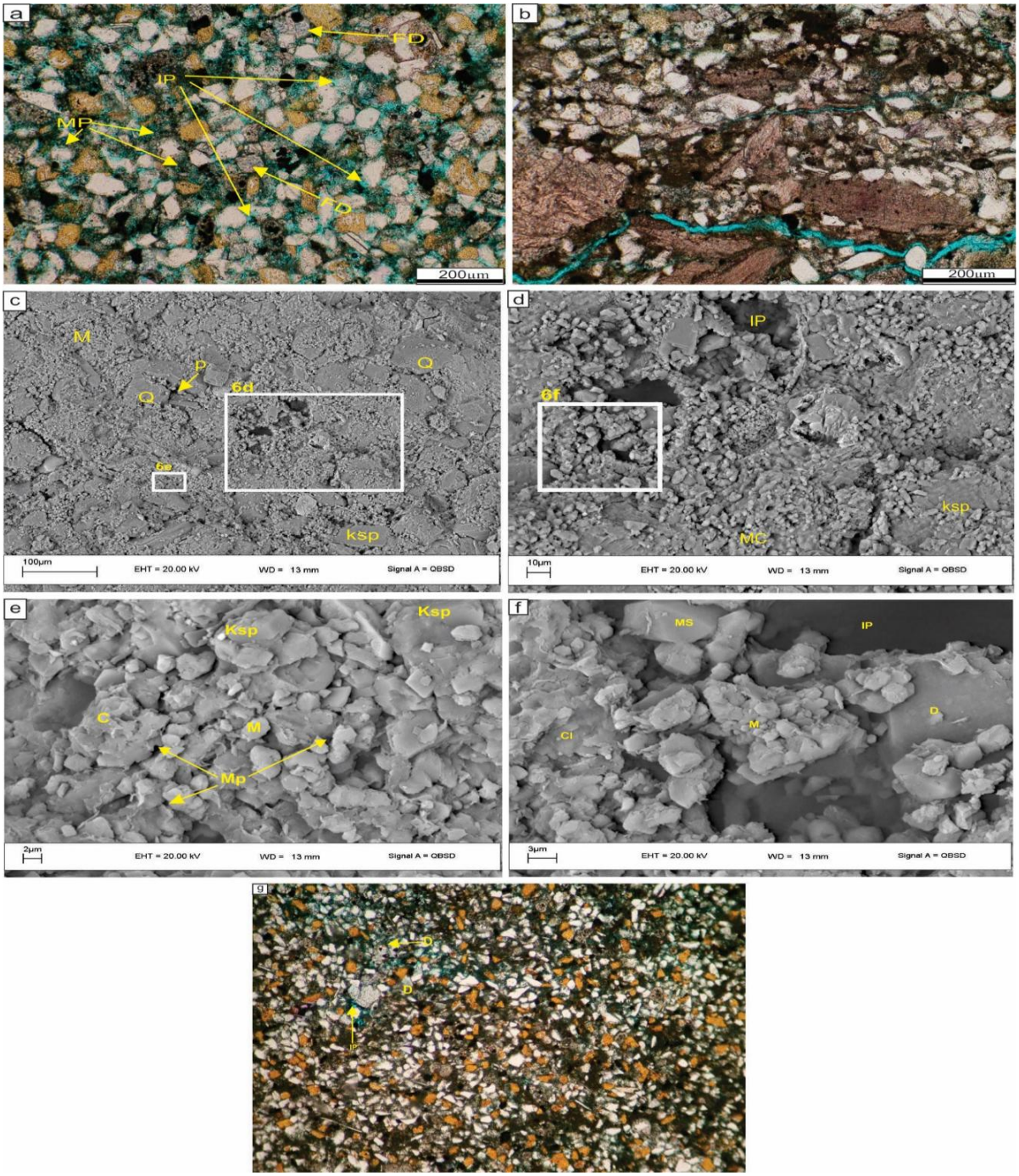

Fig. 6. (a) An area of arkosic sandstone with a relative lack of recrystallized micrite matrix, displaying local primary intergranular porosity (IP). Microporosity (Mp) is also present within the patchy clay and/or micrite/microspar matrix. Note also mildly ferroan dolomite (FD). (b) An area of sandstone which grades to the bioclastic sandstone in fig. 4b. Note the absence of intergranular porosity due to the recrystallized micritic matrix. Any apparent porosity is artefact porosity. (c) Detrital grains, quartz (Q), K feldspar (Ksp) and Ilmenite (I) not observed in thin section, in a micritic matrix (M). Scan also shows interparticle porosity (P). (d) Scan showing a general view, depicting intraparticle porosity in a planktonic foram (IP) and detrital K feldspar (Ksp) supported by a matrix composed of micrite and clays (MC). (e) A general view of detrital K feldspar (Ksp) supported by micrite (M) and clays (C). Note the microporosity (Mp). (f) Intraparticle porosity (IP) within a planktonic foraminifer test, surrounded by micrite (M), also with authigenic dolomite (D), calcite microspar (MS) and detrital flaky illitic clays (Cl). (g) A general view of the partly recrystallized micritic arkosic sandstone. Also shows very rare isolated primary intergranular porosity (IP) in an area with locally less matrix. Note the occlusion of pore space by mildly ferroan dolomite cement (D).

4.2 DIAGENETIC FEATURES

Micrite grains which recrystallized to non-ferroan calcite were dominant and micritization observed indicates allochem alteration by microbes was of a time-consuming nature. Calcite and dolomite cementation were observed along with dissolution of bioclasts as some resulting pores were infilled with either ferroan dolomite **(Fig. 4a, 6a)** or non-ferroan calcite **(Fig. 5a, 5c)**. The infills also indicate dolomitization and cementation were concomitant late stage processes. Chemical compaction is seen in point to point grain contacts, with mechanical compaction observed in deformed grain shapes, and microfractures.

4.3 POROSITY

RCA revealed sandy molluscan-metazoan-pelletal packstone as having the lowest porosity and permeability of 6.3% and 5.5mD, respectively. Despite visually estimated 1-2% secondary porosity due to a complete bioclast dissolution, low porosity and permeability could be due to the occlusion of moldic porosity by non-ferroan calcite spar mosaics which was followed by calcite cementation **(Fig. 4a)**.

Visible porosity within the partly recrystallised micritic arkosic sandstone was moderate. Its primary porosity largely occurred as patchy intergranular porosity **(Fig. 6a, 6g)**, and was visually estimated at 5% overall with traces of intraparticle porosity **(Fig. 6d, 6f)**. Unconnected secondary biomouldic porosity within the facie, visually estimated at 1-2%, developed from the complete dissolution of fragments of mollusc shells but was later partly to entirely occluded by mildly ferroan dolomite crystals **(Fig. 6g).**

Visible porosity within the slightly sandy recrystallized bioclastic wackestone was moderately high, and visually estimated at 10-15%. Primary porosity was low and occurred only as intergranular porosity (visually estimated at 3%) within the sandstone pockets which do not appear to be generally well connected **(Fig. 5b)**. Within the pockets, a patchy detrital clay matrix had occluded some primary porosity. There was a very low amount of primary intraparticle porosity within the chambers of rare foraminifera. Poorly to moderately connected moderate secondary mouldic porosity had developed from the complete to rarely incomplete dissolution of fragments of mollusc shells **(Fig. 5a, 5c, 5e)**. These pores range from <100 up to 1300μm long. A minor amount of this porosity has been occluded by non-ferroan calcite, mildly ferroan calcite and mildly ferroan dolomite crystals, with occurrence preferentially in the larger mouldic pores.

For the sandy molluscan packstone, primary porosity was largely restricted to localised intergranular porosity within the sandstone patches, where it was visually estimated at 5%, with a trace of primary intraparticle porosity within foraminifera chambers. Minor primary interparticle porosity within the packstone domains had been solution enhanced and a trace of primary intraparticle porosity had been preserved within the packstone. Moderately connected secondary mouldic porosity, visually estimated at 15%, was created from the complete dissolution of aragonitic bioclasts within the packstone **(Fig. 4c)**. Early biomoulds had been completely occluded by non-ferroan calcite spar mosaics.

Productive carbonate reservoirs are mainly characterized by secondary porosity (Esteban & Taberner, 2003), and according to Eichenseer et al., (1999), shallow burial dissolution and dolomitization are the Pinda group's carbonate reservoir porosity creation mechanisms. The porosity deductions from the analysed samples in this study is in good agreement with the earlier studies, revealing dolomitization as an efficient porosity inhibitor within the Pinda group.

V. Discussion

5.1 DEPOSITIONAL SETTING

Micritized skeletal fragments were due to low energy lagoonal sedimentation (Beigi et al., 2017). The fourth or fifth order sequences within transgressive tracts of low energy ramps were characterized by packstone and wackestone sedimentation along with a dominance of bioclastic sediments (Burchette and Wright 1992), and anoxic conditions were observed due to the lack of benthic organisms along with an assemblage of gastropod-ostracod-foraminifera and bivalves, and well preserved fish remains (Flugel 2004). Hence, the facies indicate a low energy lagoonal sedimentation dominated by anoxic and slow sedimentation conditions within the transgressive tract of the oolitic-siliciclastic ramp, with benthic rotalinid observed within the arkosic sandstone lending credence to Eichenseer et al., (1999) deduction of anoxic sediments within the ramp mixing with aerobic siliciclastic sediments derived from a delta system.

5.2 DIAGENESIS

Diagenesis was proposed as starting with the development of pyrite framboids within the micritic matrix and the chambers of foraminifera, with the pyrite later replaced by microcrystalline hematite **(Fig. 5b)**. Low temperature hydrothermal minerals like pyrite and hematite were emplaced during burial stage dissolution (Xu et al., 2017). The micritic matrix later recrystallizes to non-ferroan calcite 5μm microspar, was followed by dissolution of aragonitic shells. The next stage involved the precipitation of either blocky non ferroan medium calcite crystals or non-ferroan dolomite rhombs within the moldic pores formed from continued bioclast

dissolution. Calcite and dolomite emplacement within the study area was due to change in seawater salinity from evaporation during sea level lowering (Eichenseer et al. 1999).

5.3 RESERVOIR QUALITY

The reservoir quality was very poor for the sandy molluscan-metazoan-pelletal packstone with porosity created by biomoulds later reduced by calcite cementation. Reservoir quality within the arkosic sandstone was poor due to its widespread recrystallized microspar matrix, with a measured permeability of 20mD higher than can be explained by thin section, and microspar matrix which displays patchy microporosity. Reservoir quality was also poor within the lightly sandy recrystallized bioclastic wackestone due to the wackestone texture and low porosity, with moderate porosity occurring in the biomoulds having a permeability restricted by their poor to moderate connectivity. Reservoir quality for the sandy molluscan packstone is fair, having been generated by mollusc shell dissolution and degraded by calcite cementation. Its measured porosity of 13.9% could be due to minor microporosity within the sandstone domains.

VI. Conclusion

Petrographic analysis and SEM imaging used to describe four facies within the oolitic- siliciclastic ramp offshore Democratic Republic of Congo, revealed a prevalence of lagoon sedimentation with deltaic intercalations. Diagenetic controls on reservoir quality were found in moldic porosity occluded by calcite or dolomite cementation due to the lowering of sea levels, with detected fair reservoir quality linked to sandstone microporosity. The study provides a preliminary insight into influences of sedimentological processes on reservoir quality within the ramp for future reservoir characterization.

References

[1]. Alsharhan AS, Magara K (1995) Nature and Distribution of Porosity and Permeability in Jurassic Carbonate Reservoirs of the Arabian Gulf BAsin. Facies 32:237–253

[2]. Anka Z, Séranne M, Lopez M, et al (2009) The long-term evolution of the Congo deep-sea fan: A basin-wide view of the interaction between a giant submarine fan and a mature passive margin (ZaiAngo project). Tectonophysics 470:42–56. https://doi.org/10.1016/j.tecto.2008.04.009

[3]. Anka Z, Séranne M, Primio R di (2010) Evidence of a large upper-Cretaceous depocentre across the Continent-Ocean boundary of the Congo-Angola basin. Implications for palaeo-drainage and potential ultra-deep source rocks. Mar Pet Geol 27:601–611. https://doi.org/10.1016/j.marpetgeo.2009.08.015

[4]. Baudin F, Disnar JR, Martinez P, Dennielou B (2010) Distribution of the organic matter in the channel-levees systems of the Congo mud-rich deep-sea fan (West Africa). Implication for deep offshore petroleum source rocks and global carbon cycle. Mar Pet Geol 27:995–1010. https://doi.org/10.1016/j.marpetgeo.2010.02.006

[5]. Beglinger SE, Doust H, Cloetingh S (2012) Relating petroleum system and play development to basin evolution: West African South Atlantic basins. Mar Pet Geol 30:1–25. https://doi.org/10.1016/j.marpetgeo.2011.08.008

[6]. Beigi M, Jafarian A, Javanbakht M, et al (2017) Facies analysis, diagenesis and sequence stratigraphy of the carbonate-evaporite succession of the Upper Jurassic Surmeh Formation: Impacts on reservoir quality (Salman Oil Field, Persian Gulf, Iran). J African Earth Sci 129:179–194. https://doi.org/10.1016/j.jafrearsci.2017.01.005

[7]. Bera A, Belhaj H (2016) A comprehensive review on characterization and modeling of thick capillary transition zones in carbonate reservoirs. J Unconv Oil Gas Resour 16:76–89. https://doi.org/10.1016/j.juogr.2016.10.001

[8]. Brigaud B, Vincent B, Durlet C, et al (2014) Characterization and origin of permeability-porosity heterogeneity in shallow-marine carbonates: From core scale to 3D reservoir dimension (Middle Jurassic, Paris Basin, France). Mar Pet Geol 57:. https://doi.org/10.1016/j.marpetgeo.2014.07.004

[9]. Brownfield ME, Charpentier RR (2006) Geology and total petroleum systems of the West-Central Coastal province (7203), West Africa

[10]. Burchette TP, Wright VP (1992) Carbonate ramp depositional systems. Sediment Geol 79:3–57. https://doi.org/10.1016/0037-0738(92)90003-A

[11]. Burwood R, Cornet PJ, Jacobs L, Paulet J (1990) Organofacies variation control on hydrocarbon generation: A Lower Congo Coastal Basin (Angola) case history. Org Geochem 16:325–338. https://doi.org/10.1016/0146-6380(90)90052-2

[12]. Burwood R, De Witte SM, Mycke B, Paulet J (1995a) Petroleum Geochemical Characterisation of the Lower Congo Coastal Basin Bucomazi Formation. Springer, Berlin, Heidelberg, pp 235–263

[13]. Burwood R, Witte SM De, Mycke B, Paulet J (1995b) Petroleum Geochemical Characterisation of the Lower Congo Coastal Basin Bucomazi Formation. In: Katz B (ed) Petroleum Source Rocks. pp 235–263

[14]. Cerepi A, Barde JP, Labat N (2003) High-resolution characterization and integrated study of a reservoir formation: The danian carbonate platform in the Aquitaine Basin (France). Mar Pet Geol 20:1161–1183. https://doi.org/10.1016/j.marpetgeo.2003.09.005

[15]. Cerepi A, Humbert L, Burlot R (1999) Effects of rock-fabrics on petrophysical properties of a carbonate-rock in meteroric diagenetic zone. Bull LA Soc Geol Fr 171:419–430

[16]. Chaduteau C, Jean-Baptiste P, Fourré E, et al (2009) Helium transport in sediment pore fluids of the Congo-Angola margin. Geochemistry, Geophys Geosystems 10:1–12. https://doi.org/10.1029/2007GC001897

[17]. Charlou JL, Donval JP, Fouquet Y, et al (2004) Physical and chemical characterization of gas hydrates and associated methane plumes in the Congo-Angola Basin. Chem Geol 205:405–425. https://doi.org/10.1016/j.chemgeo.2003.12.033

[18]. Choquette PW, Pray LC (1970) Geologic Nomenclature and Classification of Porosity in Sedimentary Carbonates. Am Assoc Pet Geol Bull 54:207–250. https://doi.org/10.1306/5d25c98b-16c1-11d7-8645000102c1865d

[19]. Cole GA, Requejo AG, Ormerod D, et al (2000) Petroleum geochemical assessment of the Lower Congo Basin. AAPG Mem 73:325–339. https://doi.org/10.1306/m73705c23

[20]. Dickson WG, Fryklund RE, Odegard ME, Green CM (2003) Constraints for plate reconstruction using gravity data - Implications for source and reservoir distribution in Brazilian and West African margin basins. Mar Pet Geol 20:309–322.

https://doi.org/10.1016/S0264-8172(03)00039-4
[21]. Droz L, Rigaut F (1996) Morphology and recent evolution of the Zaire turbidite system (Gulf of Guinea). GeoScienceWorld
[22]. Dunham RJ (1962) AAPG Datapages_Archives_ Classification of Carbonate Rocks According to Depositional Textures. In: AAPG Mem. http://archives.datapages.com/data/specpubs/carbona2/data/a038/a038/0001/0100/0108.htm. Accessed 5 Apr 2020
[23]. Eagles G (2007) New angles on South Atlantic opening. Geophys J Int 168:353–361. https://doi.org/10.1111/j.1365-246X.2006.03206.x
[24]. Ehrenberg SN (2004) Factors controlling porosity in Upper Carboniferous-Lower Permian carbonate strata of the Barents Sea. Am Assoc Pet Geol Bull 88:1653–1676. https://doi.org/10.1306/07190403124
[25]. Ehrenberg SN, Aqrawi AAM, Nadeau PH (2008) An overview of reservoir quality in producing Cretaceous strata of the Middle East. Pet Geosci 14:307–318. https://doi.org/10.1144/1354-079308-783
[26]. Ehrenberg SN, Nadeau PH (2005) Sandstone vs. carbonate petroleum reservoirs: A global perspective on porosity-depth and porosity-permeability relationships. Am Assoc Pet Geol Bull 89:435–445. https://doi.org/10.1306/11230404071
[27]. Ehrenberg SN, Nielsen EB, Svånå TA, Stemmerik L (1998) Diagenesis and reservoir quality of the Finnmark carbonate platform, Barents Sea: results from wells 7128/6-1 and 7128/4-1. Nor Geol Tidsskr 78:225–252
[28]. Eichenseer HTH, Walgenwitz FR, Biondi PJ (1999) Stratigraphic control on facies and diagenesis of dolomitized oolitic siliciclastic ramp sequences (Pinda Group, Albian, Offshore Angola). Am Assoc Pet Geol Bull 83:1729–1758. https://doi.org/10.1306/e4fd4251-1732-11d7-8645000102c1865d
[29]. Embry AF, Klovan EJ (1971) A Late Devonian Reef Tract on Northeastern Bank Island, N. W. T. Bull Can Pet Geol 19:730–781
[30]. Esteban M, Taberner C (2003) Secondary porosity development during late burial in carbonate reservoirs as a result of mixing and/or cooling of brines. J Geochemical Explor 78–79:355–359. https://doi.org/10.1016/S0375-6742(03)00111-0
[31]. Flugel E (2004) Microfacies of Carbonate Rocks. Springer Berlin Heidelberg, New York
[32]. Franks S, Nairn AEM (1973) The Equatorial Marginal Basins of West Africa. In: The South Atlantic. Springer US, pp 301–350
[33]. Frixa A, Maragliulo C, Consonni A, Ortenzi A (2014) Dolomitization of the lacustrine carbonates of the Toca Fm. (Kambala field, offshore Cabinda) and quantitative diagenetic modeling. Soc Pet Eng - 30th Abu Dhabi Int Pet Exhib Conf ADIPEC 2014 Challenges Oppor Next 30 Years 4:3017–3030. https://doi.org/10.2118/171960-ms
[34]. Ge Z, Gawthorpe RL, Rotevatn A, et al (2019) Minibasin depocentre migration during diachronous salt welding, offshore Angola. Basin Res. https://doi.org/10.1111/bre.12404
[35]. Holtvoeth J, Wagner T, Schubert CJ (2003) Organic matter in river-influenced continental margin sediments: The land-ocean and climate linkage at the Late Quaternary Congo fan (ODP Site 1075). Geochemistry, Geophys Geosystems 4:. https://doi.org/10.1029/2003GC000590
[36]. Holtz MH, Ruppel SC, Hocott CR (1992) Integrated geologic and engineering determination of oil-reserve-growth potential in carbonate reservoirs. JPT, J Pet Technol 44:1250–1257. https://doi.org/10.2118/22900-PA
[37]. Hosa A, Wood R (2017) Quantifying the impact of early calcite cementation on the reservoir quality of carbonate rocks: A 3D process-based model. Adv Water Resour 104:89–104. https://doi.org/10.1016/j.advwatres.2017.02.019
[38]. Huang Y (2018) Sedimentary characteristics of turbidite fan and its implication for hydrocarbon exploration in Lower Congo Basin. Pet Res 3:189–196. https://doi.org/10.1016/j.ptlrs.2018.02.001
[39]. J.Vidal, Joyes R, Veen J Van (1975) L'exploration petroliere au Gabon et au Congo. New Oil Gas Bear Areas Outs Far East 8:149–166
[40]. Jameson M, Wells S, Greenhalgh J, Borsato R (2011) Prospectivity and seismic expressions of pre- and post-salt plays along the conjugate margins of Brazil, Angola and Gabon. Soc Explor Geophys Int Expo 81st Annu Meet 2011, SEG 2011 1062–1067. https://doi.org/10.1190/sbgf2011-160
[41]. Jansen JH., Giresse P, Moguedet G (1984) Structural and Sedimentary Geology of the Congo and Southern Gabon Continental Shelf; A Seismic and Acoustic Reflection Survey. Netherlands J Sea Res 17:364–384
[42]. Jardine D, Wilshart JW (1982) Carbonate Reservoir Description. In: International Petroleum Exhibition and Technical Symposium. Society of Petroleum Engineers
[43]. Jatiault R, Dhont D, Loncke L, Dubucq D (2017) Monitoring of natural oil seepage in the Lower Congo Basin using SAR observations. Remote Sens Environ 191:258–272. https://doi.org/10.1016/j.rse.2017.01.031
[44]. Jiang L, Hu S, Zhao W, et al (2018) Diagenesis and its impact on a microbially derived carbonate reservoir from the middle triassic leikoupo formation, Sichuan Basin, China. Am Assoc Pet Geol Bull 102:2599–2628. https://doi.org/10.1306/05111817021
[45]. Lavoie D, Chi G (2001) The lower Silurian Sayabec formation in northern gaspé: Carbonate diagenesis and reservoir potential. Bull Can Pet Geol 49:282–298. https://doi.org/10.2113/49.2.282
[46]. Lentini MR, Fraser SI, Scott Sumner H, Davies RJ (2010) Geodynamics of the central South Atlantic conjugate margins: Implications for hydrocarbon potential. Pet Geosci 16:217–229. https://doi.org/10.1144/1354-079309-909
[47]. Leturmy P (2003) Dynamic interactions between the gulf of Guinea passive margin and the Congo River drainage basin: 1. Morphology and mass balance. J Geophys Res 108:1–13. https://doi.org/10.1029/2002jb001927
[48]. Li Q, Wu W, Liang J, et al (2020) Deep-water channels in the lower Congo basin: Evolution of the geomorphology and depositional environment during the Miocene. Mar Pet Geol 115:104260. https://doi.org/10.1016/j.marpetgeo.2020.104260
[49]. Liu JP, Pan X hua, Ma J, et al (2008) Petroleum geology and resources in West Africa: An overview. Pet Explor Dev 35:378–384. https://doi.org/10.1016/S1876-3804(08)60086-5
[50]. Liu Z, Li J (2011) Control of salt structures on hydrocarbons in the passive continental margin of West Africa. Pet Explor Dev 38:196–202. https://doi.org/10.1016/S1876-3804(11)60025-6
[51]. Machel HG, Buschkuehle BE (2008) Diagenesis of the Devonian Southesk-Cairn Carbonate Complex, Alberta, Canada: Marine Cementation, Burial Dolomitization, Thermochemical Sulfate Reduction, Anhydritization, and Squeegee Fluid Flow. J Sediment Res 78:366–389. https://doi.org/10.2110/jsr.2008.037
[52]. Madi A, Savard MM, Bourque PA, Guoxiang C (2000) Hydrocarbon potential of the Mississippian carbonate platform, Bechar basin, Algerian Sahara. Am Assoc Pet Geol Bull 84:266–287. https://doi.org/10.1306/c9ebcdc9-1735-11d7-8645000102c1865d
[53]. Major RP, Holtz MH (1997) Predicting Reservoir Quality at the Development Scale: Methods for Quantifying Remaining Hydrocarbon Resource in Diagenetically Complex Carbonate Reservoirs. In: Kupecz JA, Gluyas J, Bloch S (eds) Reservoir quality prediction in sandstones and carbonates: AAPG Memoir. pp 231–248
[54]. Marcano G, Anka Z, di Primio R (2013) Major controlling factors on hydrocarbon generation and leakage in South Atlantic conjugate margins: A comparative study of Colorado, Orange, Campos and Lower Congo basins. Tectonophysics 604:172–190. https://doi.org/10.1016/j.tecto.2013.02.004
[55]. Mazzullo SJ (1994) Diagenesis in a sequence-stratigraphic setting: porosity evolution in periplatform carbonate reservoirs, Permian Basin, Texas and New Mexico. J Pet Sci Eng 11:311–322. https://doi.org/10.1016/0920-4105(94)90049-3

[56]. Mehrabi H, Rahimpour-Bonab H (2014) Paleoclimate and tectonic controls on the depositional and diagenetic history of the Cenomanian-early Turonian carbonate reservoirs, Dezful Embayment, SW Iran. Facies 60:147–167. https://doi.org/10.1007/s10347-013-0374-0
[57]. Moulin M, Aslanian D, Olivet JL, et al (2005) Geological constraints on the evolution of the Angolan margin based on reflection and refraction seismic data (ZaïAngo project). Geophys J Int 162:793–810. https://doi.org/10.1111/j.1365-246X.2005.02668.x
[58]. Moulin M, Aslanian D, Unternehr P (2010) A new starting point for the South and Equatorial Atlantic Ocean. Earth-Science Rev. 98:1–37
[59]. Nader FH, Swennen R (2004) Petroleum prospects of Lebanon: Some remarks from sedimentological and diagenetic studies of Jurassic carbonates. Mar Pet Geol 21:427–441. https://doi.org/10.1016/S0264-8172(03)00095-3
[60]. Nürnberg D, Müller RD (1991) The tectonic evolution of the South Atlantic from Late Jurassic to present. Tectonophysics 191:27–53. https://doi.org/10.1016/0040-1951(91)90231-G
[61]. Oluboyo AP, Gawthorpe RL, Bakke K, Hadler-Jacobsen F (2014) Salt tectonic controls on deep-water turbidite depositional systems: Miocene, southwestern Lower Congo Basin, offshore Angola. Basin Res 26:597–620. https://doi.org/10.1111/bre.12051
[62]. Rahimpour-Bonab H, Esrafili-Dizaji B, Tavakoli V (2010) Dolomitization and anhydrite precipitation in permo-triassic carbonates at the south Pars gasfield, offshore Iran: Controls on reservoir quality. J Pet Geol 33:43–66. https://doi.org/10.1111/j.1747-5457.2010.00463.x
[63]. Rashid F, Glover PWJ, Lorinczi P, et al (2017) Microstructural controls on reservoir quality in tight oil carbonate reservoir rocks. J Pet Sci Eng 156:814–826. https://doi.org/10.1016/j.petrol.2017.06.056
[64]. Rouby D, Guillocheau F, Robin C, et al (2003) Rates of deformation of an extensional growth fault/raft system (offshore Congo, West African margin) from combined accommodation measurements and 3-D restoration. Basin Res 15:183–200. https://doi.org/10.1046/j.1365-2117.2003.00200.x
[65]. Ruiter PAC de (1979) The Gabon and Congo Basins Salt Deposits. Econ Geol 74:419–431
[66]. Saller AH, Budd DA, Harris PM (1994) Unconformities and porosity development in carbonate strata: ideas from a Hedberg Conference. Am Assoc Pet Geol Bull 78:857–871. https://doi.org/10.1306/a25fe3c9-171b-11d7-8645000102c1865d
[67]. Salvi F, Tsikalas F, Lottaroli F, et al (2013) Crustal-scale architecture and heat flow account in ultra-deep water lower Congo basin. Soc Pet Eng - Int Pet Technol Conf 2013, IPTC 2013 Challenging Technol Econ Limits to Meet Glob Energy Demand 5:3784–3788
[68]. Schlager W (1999) Sequence stratigraphy of carbonate rocks
[69]. Scholle PA (1978) A colour guide to carbonates: Carbonate Rock Constituents, Textures, Cements, and Porosities. AAPG Mem 27:1–241. https://doi.org/10.1016/j.idc.2015.02.006
[70]. Séranne M, Anka Z (2005) South Atlantic continental margins of Africa: A comparison of the tectonic vs climate interplay on the evolution of equatorial west Africa and SW Africa margins. J African Earth Sci 43:283–300. https://doi.org/10.1016/j.jafrearsci.2005.07.010
[71]. Singh KH, Joshi RM (2020) Petro-physics and Rock Physics of Carbonate Reservoirs. Springer Singapore
[72]. Torsvik TH, Rousse S, Labails C, Smethurst MA (2009) A new scheme for the opening of the South Atlantic Ocean and the dissection of an Aptian salt basin. Geophys J Int 177:1315–1333. https://doi.org/10.1111/j.1365-246X.2009.04137.x
[73]. Uchupi E, Emery KO (1975) Continental Margin Off Western Africa: Angola to Sierra Leone. Am Assoc Pet Geol Bull 59:2209–2265. https://doi.org/10.1306/83d92249-16c7-11d7-8645000102c1865d
[74]. Uenzelmann-Neben G, Spiess V, Bleil U (1997) A seismic reconnaissance survey of the northern Congo Fan. Mar Geol 140:283–306. https://doi.org/10.1016/S0025-3227(97)00045-5
[75]. Valle PJ, Gjelberg JG, Helland-Hansen W (2001) Tectonostratigraphic development in the Eastern Lower Congo Basin, offshore Angola, West Africa. Mar Pet Geol 18:909–927. https://doi.org/10.1016/S0264-8172(01)00036-8
[76]. Vandeginste V, Swennen R, Reed MH, et al (2009) Host rock dolomitization and secondary porosity development in the Upper Devonian Cairn Formation of the Fairholme carbonate complex (South-west Alberta, Canadian Rockies): Diagenesis and geochemical modelling. Sedimentology 56:2044–2060. https://doi.org/10.1111/j.1365-3091.2009.01069.x
[77]. Wang L, Wang Z, Yu S, Ngia NR (2016) Seismic responses and controlling factors of Miocene deepwater gravity-flow deposits in Block A, Lower Congo Basin. J African Earth Sci 120:31–43. https://doi.org/10.1016/j.jafrearsci.2016.04.015
[78]. Wenau S, Spiess V, Pape T, Fekete N (2015) Cold seeps at the salt front in the Lower Congo Basin II: The impact of spatial and temporal evolution of salt-tectonics on hydrocarbon seepage. Mar Pet Geol 67:880–893. https://doi.org/10.1016/j.marpetgeo.2014.09.021
[79]. Wennberg OP, Casini G, Jonoud S, Peacock DCP (2016) The characteristics of open fractures in carbonate reservoirs and their impact on fluid flow: A discussion. Pet Geosci 22:91–104. https://doi.org/10.1144/petgeo2015-003
[80]. Wierzbicki R, Dravis JJ, Al-Aasm I, Harland N (2006) Burial dolomitization and dissolution of Upper Jurassic Abenaki platform carbonates, Deep Panuke reservoir, Nova Scotia, Canada. Am Assoc Pet Geol Bull 90:1843–1861. https://doi.org/10.1306/03200605074
[81]. Wilson MEJ, Evans MJ, Oxtoby NH, et al (2007) Reservoir quality, textural evolution, and origin of fault-associated dolomites. Am Assoc Pet Geol Bull 91:1247–1272. https://doi.org/10.1306/05070706052
[82]. Woody RE, Gregg JM, Koederitz LF (1996) Effect of texture on petrophysical properties of dolomite: Evidence from the Cambrian-Ordovician of southeastern Missouri. Am Assoc Pet Geol Bull 80:119–132. https://doi.org/10.1306/64ed8764-1724-11d7-8645000102c1865d
[83]. Xu S, Bi H, Li S, et al (2017) Deep burial dissolution of Lower Palaeozoic carbonates and the role of compacted released water from Palaeogene strata in the Zhuanghai area, Jiyang Depression, Bohai Bay Basin, NE China. Geol J 52:30–44. https://doi.org/10.1002/gj.2730
[84]. Zhou X, Ding W, He J, et al (2018) Microfractures in the middle Carboniferous carbonate rocks and their control on reservoir quality in the Zanaral Oilfield. Mar Pet Geol 92:462–476. https://doi.org/10.1016/j.marpetgeo.2017.11.009
[85]. Zou C, Tao S (2007) Major factors controlling the formation of middle and large marine carbonate stratigraphic fields. Chinese Sci Bull 52:44–53. https://doi.org/10.1007/s11434-007-6011-y

Nadège Mbula Ngoy, et. al. "Petrographic and Diagenetic Evaluation of Carbonate Reservoir Quality: A Case study of the Lower Congo Basin, offshore Democratic Republic of Congo." *IOSR Journal of Applied Geology and Geophysics (IOSR-JAGG)*, 8(5), (2020): pp 15-26.